

# Assessment of a preclinical model for studying the survival and engraftment of human stem cell derived osteogenic cell populations following orthotopic implantation

J.L. Tremoleda<sup>2,4</sup>, N.S. Khan<sup>4</sup>, V. Mann<sup>1,4</sup>, S.N. Racey<sup>3,4</sup>, A.J. Martin<sup>4</sup>, A.H.W.R. Simpson<sup>4</sup>, B.S. Noble<sup>1,4</sup>

<sup>1</sup>School of Science, Technology and Health, University Campus Suffolk, Waterfront Building, 19 Neptune Quay, Ipswich IP4 1QJ;

<sup>2</sup>Biological Imaging Centre, MRC Clinical Science Centre, Imperial College London, Hammersmith Campus, London W12 0NN;

<sup>3</sup>School of Applied Sciences, Northumbria University, Ellison Building, Newcastle upon Tyne NE1 8ST;

<sup>4</sup>College of Medicine and Veterinary Medicine, University of Edinburgh, 49 Little France Crescent, Edinburgh, EH16 4SB

## Abstract

**Introduction:** Preclinical studies with osteoprogenitor cells derived from human embryonic stem cells (hESC) do not lead to substantial bone regeneration *in vivo*. The degree of survival following implantation might play a role in their long term efficiency. We investigated the initial engraftment of hESCs-derived cells during two weeks post-implantation and compared it to such response for adult bone marrow stromal cells (hBMSC)-derived osteoprogenitor cells. **Methods:** hBMSC and H9-hES cells pretreated with osteogenic factors were implanted into a calvarial defect in both adult WT and nude rats. At days 7 and 14 post-implantation, samples were analysed for persistence of implanted cells, initiation of regeneration of host bone, angiogenesis and apoptosis. **Results:** At day 7, hESC and hBMSC were detected within defects in both rat strains. By day 14 human cells were only detected in immune-deficient rats whilst still maintaining an osteoblastic phenotype and engendered a significant increase in bone formation. In WT animals, the participation of implanted cells was very limited due to their poor survival. **Conclusion:** This study demonstrates the ability of hESC and hBMSC derived osteoprogenitor cells to survive transplantation, to engraft and to develop an osteogenic phenotype during the early stage following implantation, validating the appropriate preclinical model.

**Keywords:** Bone Regeneration, Osteoprogenitors, Stem Cells, Transplantation, Calvarial Model

## Introduction

Musculoskeletal diseases are a major cause of disability and represent a substantial socio economic burden for healthcare authorities worldwide. Current treatments for bone deficien-

cies arising from acute trauma, tumor resection or genetic disorders provide limited functional recovery associated with the poor regenerative potential of the diseased bone and inadequacy of tissue incorporation in injured/diseased areas<sup>1-3</sup>. The efficacy of current treatments is limited by the availability of grafting material and the poor biocompatibility and inadequate mechanical properties of the biomaterials used. Demand for alternative treatments is high and the search for cell based therapies is emerging as a large scale effort worldwide.

Major advances are being made in the field of stem cell biology and tissue engineering that point to the development of stem cell derived therapies to the clinic<sup>4-7</sup>. In particular, protocols for the efficient differentiation of committed and functional somatic cells from stem cell sources are available. Bone-forming cells can be obtained from adult derived bone marrow stromal cells (hBMSCs<sup>8</sup>) and these cells have been reported to successfully enhance repair in critical/non-healing bone defects following autologous transplantation<sup>9,10</sup>. However, the restricted ability of hBMSCs to proliferate *in vitro* and to maintain their

The authors have no conflict of interest.

### Corresponding authors:

Prof. Brendon Noble, Head of School, School of Science, Technology and Health, University Campus Suffolk, Waterfront Building, 19 Neptune Quay, Ipswich IP4 1QJ

E-mail: b.noble@ucs.ac.uk

Dr Jordi L.Tremoleda, Biological Imaging Centre, MRC Clinical Science Centre, Imperial College London, Hammersmith Campus, London W12 0NN

E-mail: jordi.lopez-tremoleda@imperial.ac.uk

Edited by: F. Rauch

Accepted 21 October 2012

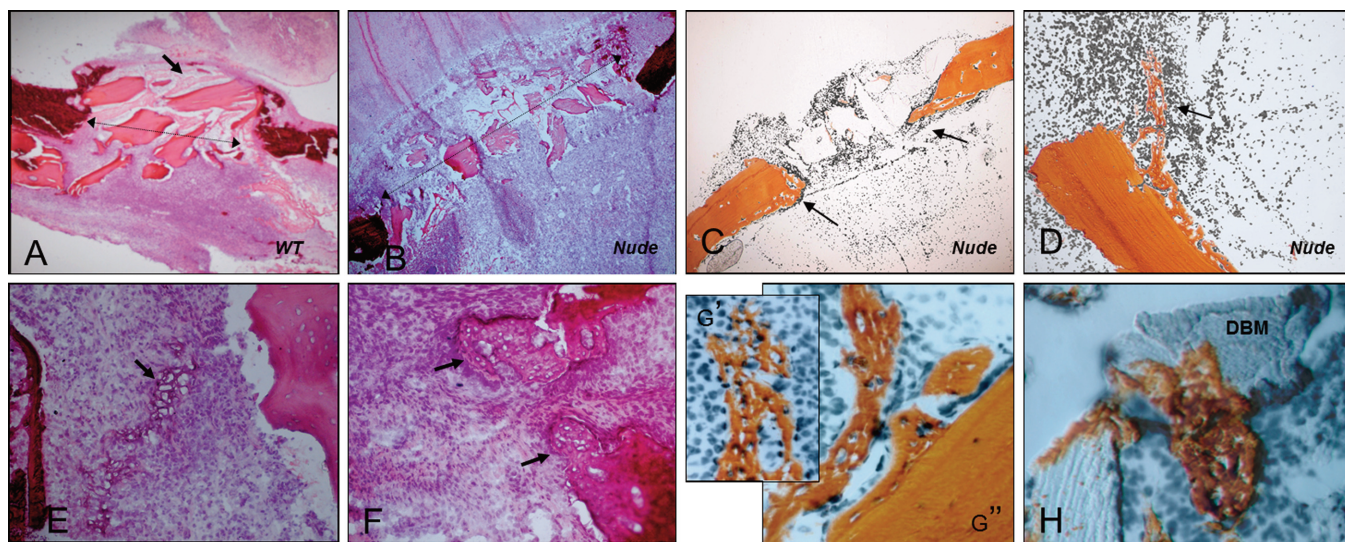


**Figure 1.** H&E or Von Kossa stained cryosections of calvarial defect: **A)** Loosely organised tissue with large areas of fibrin glue deposits detected in day 7 implanted hESCs OS-derived cells in a WT rat (H&E  $\times 40$ ); **B)** Day 7 implanted hESCs OS-derived cells in a nude rat (H&E  $\times 40$ ); **C)** Areas of bone regeneration mostly in the inner pericranial edges of the parietal bone (*arrows*) detected in a day 14 implanted hBMSC OS-derived cells in a nude rat (Von Kossa  $\times 40$ ); **D)** Areas of bone regeneration displayed as woven bone with large cellular activity (*arrow*) in a day 7 implanted hMSC OS-derived cells in a nude rat (Von Kossa  $\times 100$ ); **E)** New osteoid produced by osteoprogenitor cells within the defect and **F)** in the edges of the rat calvarial bone in a day 14 implanted hESC OS derived cells in a nude rat (H&E  $\times 200$ ); **G)** Areas of newly laid and growing areas of mineralised woven bone in the edges of the defect in a day 14 implanted hESC OS-derived cells in a nude rat (Von Kossa  $\times 400$ ); **G'**: displays large number of osteoprogenitor cells (Dapi labelled) integrated within the new mineralized woven bone. **H)** Bony regenerate forming along and bridging towards the DBM particles in a day 14 implanted hESC OS derived cells in a nude rat ( $\times 400$ ); WT (wild-type), DBM (Demineralised bone matrix).

osteogenic potential<sup>11</sup>, along with the fact that these cells are limited in number and only form a small proportion of the initial isolated culture could hinder their production at a scale sufficient to be of use in clinical applications. Human embryonic stem cells (hESCs) offer the theoretical advantage of unlimited supply of multipotential cells due to their high proliferation and self renewal capacity. Previous studies have demonstrated the directed differentiation of hESCs down the osteogenic lineage resulting in the formation of bone-forming osteoblasts *in vitro*<sup>12,13</sup> and within ectopic sites<sup>13,14</sup> or orthotopic site<sup>15,16</sup> *in vivo*. However, *in vivo* studies have shown inconsistent results on bone formation, showing only limited mineralized deposits, presence of dystrophic calcification, survival and engraftment of implanted cells and very limited information on the *in situ* response in the implanted host tissue<sup>17</sup>. The translation of bench findings into clinical therapeutic protocols requires extensive, preclinical examination in appropriate animal models.

The rational approaches for the use of animal models to assess bone regeneration demand the creation of a reproducible environment that is as close as possible to the clinical setting in which the therapy will be used. These include the use of animal models that will provide an *in vivo* physiological responsiveness comparable to that in humans; the creation of a lesion that closely resembles the anatomical location and function of the tissue to be repaired and the development of an appropriate delivery system in a manner in which it has measurable and observable effects.

Rodents have provided an effective setting for screening for evidence of stem cells or progenitor cell homing to sites of bone repair, and the cranial defects are considered to be relatively reproducible model for osteogenesis<sup>18</sup>. Transplantation of cultured hBMSCs with a mineral matrix has been successfully used to promote the healing of a calvarial defect in a pre-clinical animal model<sup>19</sup>. With the development of protocols to efficiently direct the differentiation of hESCs to osteoblast, we need to elucidate further clues to ensure consistent bone formation when implanted *in vivo*. The mechanism of regeneration in animal models may be afforded in the presence but also in absence of implanted cells after long term implants. This possibility results in difficulties in experimental interpretation and reduces predictive value in relation to implantation in the human patient. While most of the *in vivo* studies have focused on the final outcome at late stages of implantation<sup>15-17</sup>, we decided to investigate the early *in situ* response following implantation of hESC-derived cells. It is important to address the likelihood of the differentiated hESC derived cells to be immune rejected and their initial response to a hostile injured environment to assess their therapeutic potential for bone repair before engaging into longer term pre-clinical studies. We examined the ability of osteoprogenitor cells derived from both hBMSC and hESC to survive, engraft and maintain a differentiated state to support tissue repair after implantation in a calvarial bone defect in immunocompetent and immunocompromised rats over a two week period.

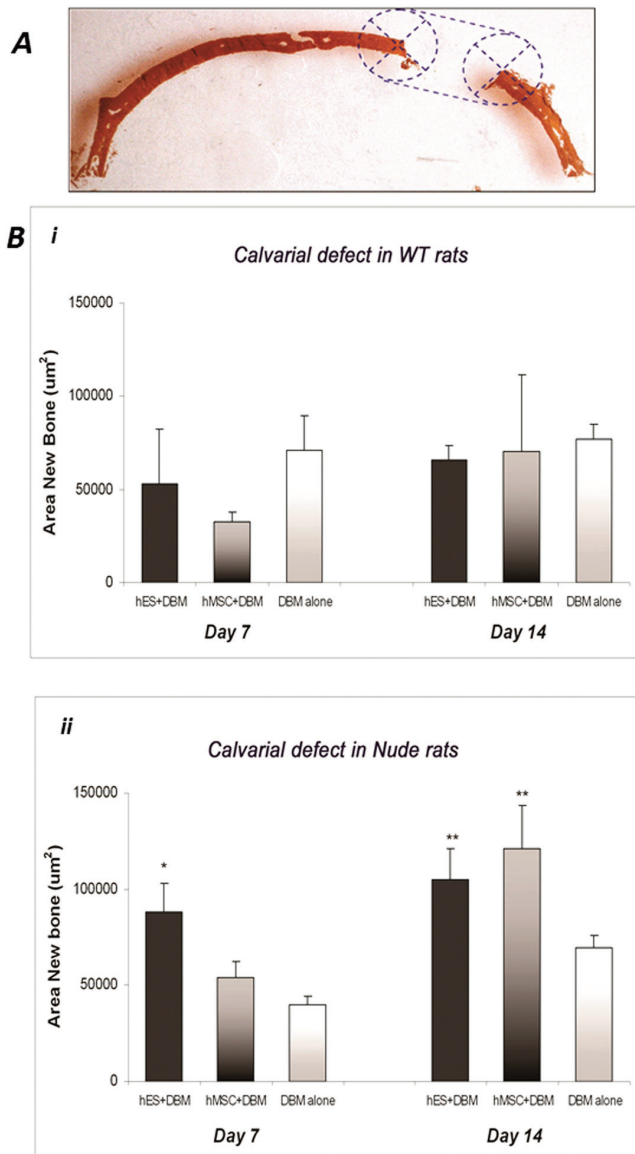


**Figure 2.** Histomorphometric analysis of mineralization. **A)** Von-kossa stained calvarial cryosection displaying a representation of the graticule used for the histomorphometric analysis ( $\times 40$ ). **B)** Analysis of newly generated bone tissue in calvarial defect post-implantation of hESC or hBMCS-derived cells with DBM or DBM alone in nude and WT rats for 7 and 14 days. **i)** No significant differences were detected for WT rats implanted with hESC or hBMSC-derived cells with DBM or DBM alone after 7 or 14 days. **ii)** Total area of newly mineralised tissue (mean $\pm$ SEM) was significantly increased in calvarial defect implanted with hESC/DBM at day 7 ( $P=0.003$ ). By day 14, implantation of hESC and hBMSC-derived cells with DBM significantly increased the area of new bone formed ( $P=0.02$ ). (ANOVA with post-hoc comparison by Bonferroni test;  $P<0.05$ ; superscripts denote significant differences between groups per implantation time).

## Materials and methods

### Cell culture

The human embryonic stem cell line H9 (Madison, WI)<sup>20</sup> was used in this study. Of all hESC lines reported in the literature, H9 (including their derivatives) are among the cell lines most frequently used in international research<sup>21</sup>. hES cells were cultured following minor modifications to an established protocol<sup>22</sup>. Cells were grown in flasks coated with Matrigel (Becton Dickinson, USA), and maintained in conditioned serum free growth media (CGM). Basal serum-free growth medium ('GM') comprised KO-DMEM (Gibco, UK) supplemented with 20% Serum Replacement (Gibco), 1 mM L-Glutamine (Gibco), 1% non essential amino acids (Gibco), 100 mM  $\beta$ -mercaptoethanol (Gibco) and 4 ng/ml bFGF (Sigma-Aldrich, UK). Prior to use with hES cells GM was conditioned by incubation for 24 hours with subconfluent cultures of mouse embryonic fibroblasts. Conditioned GM was supplemented further with 4 ng/ml bFGF and filtered to create the conditioned growth medium ('CGM') used for hES cell culture. Cells were maintained at 37°C in a humid 5% CO<sub>2</sub> atmosphere. Differentiation protocols have been described previously<sup>12</sup>. Briefly, H9 cells were enzymatically disaggregated with Trypsin-EGTA<sup>23</sup> and embryoid bodies (EBs) formed by placing cells in suspension culture for 48 hours at which point CGM was removed and replaced with Embryoid Body Medium ('EBM' comprising KO-DMEM supplemented with 10% FCS (GlobePharm Ltd, UK), 1 mM L-Glutamine, 1% non essential amino acids and 100 mM  $\beta$ -mercapto ethanol). After a further 2-3 days, EBs were trypsinized and EB cells plated on 0.1% gelatin coated tissue culture plastic.

Adult human bone marrow stromal cells (hBMSC) were harvested from femoral head tissue obtained under informed consent, and with the approval of the local ethical committee, from patients undergoing arthroplasty. Bone marrow stromal cells were prepared as previously described<sup>24</sup>. Briefly, whole bone marrow was removed from femoral heads, titrated and cultured in DMEM supplemented with 10% FCS, L-glutamine (2 mM), penicillin (100 IU/ml) and streptomycin (100  $\mu$ /ml). Bone marrow cells were maintained at 37°C in humidified 5% CO<sub>2</sub> atmosphere undisturbed for 4 days after which time non-adherent cells were removed and fresh growth media added to the adherent cell population. Primary isolates of adherent MSC were maintained in culture until confluent, washed 3x in PBS and passaged using 0.05% trypsin in PBS solution. hBMSC cultures were used between passage 2-4 and their phenotype routinely characterised by flow cytometry ( $\approx$ 90% CD105 positive cells).

### Osteogenic differentiation and cell preparation for implantation

Pre-treatment of hESCs and hBMSCs with osteogenic factors *in vitro* for a 4 day period has been shown to efficiently direct their osteogenic differentiation prior to implantation<sup>14</sup>.

Base media ('EBM' for hESCs and 'supplemented DMEM' for hBMSCs) supplemented with 50  $\mu$ M ascorbic acid phosphate (Wako, Germany), 10 mM  $\beta$ -glycerophosphate (Sigma-Aldrich, UK) and 100 nM dexamethasone (Sigma-Aldrich) was

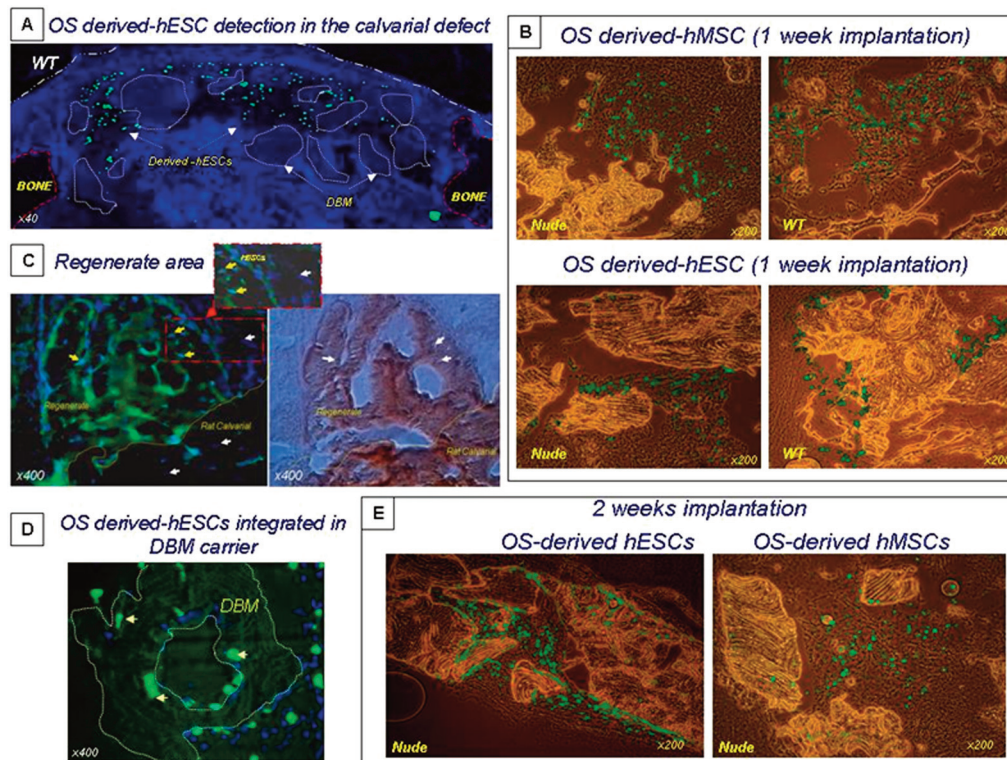


**Figure 3.** Identification of implanted human ESC and MSC-derived osteoprogenitor cells: green fluorescent signal shows hybridisation of the human DNA specific probe to DNA of implanted human cells. **A)** microphotograph of a whole cryosection of a calvarial defect in a WT rat after 7 day implantation of hESC OS derived cells. Human cells (green) are detected throughout the whole defect area. DAPI is used as a nuclear counterstain to detect rat and human cells. Highlights show the edges of the calvarial bone and the DBM particles. (*x40*). **B)** Day 7 implanted hESC and hMSC OS-derived cells in nude and WT rats. Human cells (green)/DBM and boney structures visualised by phase contrast field (*x200*). **C)** Detection of human implanted cells, depicted as merged green (human probe) and blue labeling (DAPI), embedded within the boney regenerate (Von kossa stained) in the edges of the defect. In a nude rat day 14 post implantation of hESC-OS derived cells (*x400*). **D)** Close-up view to display the close contact of OS-derived hESC cells with DBM particles after 14 days of implantation. (*x400*). **E)** Day 14 implanted hESC and hMSC OS-derived cells in nude and WT rat. Human cells are identified scattered in the defect area, integrated with DBM particles and in the regenerating edges of the calvarial bone (*x200*).

added to the cell cultures for 4 days prior to implantation to direct the osteogenic differentiation of both hBMSCs and hESCs. After 4 days in this osteogenic supplemented (OS) media the cells were harvested using 0.05% trypsin in PBS for hBMSC or trypsin-EGTA for hESC, PBS washed and re-suspended in 40  $\mu$ l of growth media at a density of  $3 \times 10^8$  cells/ml The cell suspension was mixed with 4 mg of demineralised human bone matrix (DBM: Allosource<sup>®</sup>, Centennial, USA) prior to application *in vivo*, following previous study on reconstruction of rat calvarial defects by Gurevitch et al. (2003)<sup>25</sup>.

#### *In vivo* implantation

Adult three months old male Sprague-dawley rats (immunocompetent wild type) and *RNU-Foxn1<sup>tm1</sup>* nude rats (immunocompromised type) (Harlan UK limited, <http://www.harlan.com>) were used in this study. All animals were maintained under the guidelines set by the institutional Animal Care and Ethical Committee at the University of Edinburgh, and the procedures approved

under a UK Home Office license. All operations were performed under general anaesthesia (2-3.5% isoflurane) and with fixed skull orientation using a Lab standard<sup>™</sup> stereotaxic frame (Stoeling Co, USA). The calvarial periosteum was removed from the skull and a 6 mm diameter full thickness cranial defect was created laterally in the right nonsuture-associated parietal bone under constant irrigation, avoiding any trauma to the underlying dura mater and to the meningeal vessels underneath the sagittal suture. Either OS-pretreated hES or hBMSC cells in DBM or DBM alone (control group) were implanted for either 7 days or 14 days into the calvarial defect in immunocompetent (wild type) and in immunocompromised (nude) rats (total 36 animals; n=3 per experimental group). Implants were sealed with fibrin glue (Tisseel<sup>®</sup>, Baxter Healthcare Ltd, UK).

#### *Histological Examination*

At day 7 and 14 the animals were sacrificed and calvaria dissected and flash frozen in super cooled (-80°C) hexane. 7

$\mu\text{m}$  transverse cryosections of calvariae were prepared and fixed in 4% (w/v) paraformaldehyde. To investigate the survival of implanted human cells and the *in situ* cellular response, including vascularity, apoptosis and initiation of bone regeneration within the defect site, representative cryosections (between 3 and 5, see below) were collected from the margins and the centre of the defect.

#### Identification of human implanted cells

Visualisation of human cells in the rodent lesion provides a good indicator of implant cell survival and distribution. Implanted hBMSC and hES derived osteoprogenitor cells were identified using fluorescence *in situ* hybridization (FISH) for human DNA following a protocol adapted from Newsome et al.<sup>26</sup>. Briefly, total human genomic DNA was labeled with digoxigenin 11-UTP (Roche Diagnostics Ltd, UK) by nick translation. Specific activity of the probes was performed by dotting onto nitrocellulose filters using anti-digoxigenin-alkaline phosphatase Fab fragments (Roche Diagnostics Ltd) and the reaction was visualised by using a BCIP/NBT kit (Vector Laboratories Ltd., UK) which gives a colour change on the filter for comparison with a DNA concentration standard curve.

Cryosections were fixed in 4% paraformaldehyde, washed 3X in PBS, decalcified by incubation in 50 mM Tris-HCl; 0.25 M EDTA pH 7.4 solution and in 0.1 M Tris Acetate pH 7.3 solution both for 10 min and washed thoroughly. Sections were then microwaved for 20 minutes in 10 mM Citrate buffer (pH 6.0), cooled, washed in 2X sodium saline citrate (SSC), denatured for 3 minutes at 75°C in 70% formamide/2X SSC, plunged into ice cold 70% ethanol and dehydrated through an alcohol series followed by air drying.

The human probe was prepared by mixing 30  $\mu\text{l}$  of hybridisation buffer: (50% formamide 2X SSC 10% Dextran Sulphate 1% Tween) with 150 ng of labeled human genomic DNA and 5  $\mu\text{g}$  of fish sperm DNA (Roche Diagnostics Ltd). The probe mixture was then denatured for 5 minutes at 75°C and then re-annealed at 37°C for 30 minutes. Cryosections were then incubated overnight with the probe mixture at 37°C in a humidified chamber. Unbound probe was washed off in 2X SSC at 45°C followed by a high stringency wash of 0.1X SSC at 60°C. The hybridised probe was then detected using immunocytochemistry. Briefly, slides were blocked in 4X SSC 5% milk powder (Marvel) and incubated with Sheep anti-Dig primary antibody (1:50; Roche Diagnostics Ltd.) and Alexa 488 anti sheep secondary antibody (1:200; Molecular Probes®). Slides were washed in 4X SSC 0.1% Tween after each antibody step. Sections were counterstained with DAPI (2  $\mu\text{g}/\text{ml}$  in PBS) and mounted in Dako Fluorescent Mounting Medium (Dakocytomation Ltd, UK).

#### Characterisation of human osteogenic phenotype in the rodent host by RNA isolation and reverse transcription-polymerase chain reaction (RT-PCR)

Maintenance of the osteogenic differentiation state in the host will be critical to the development of a therapy. In order to establish the presence of human cells with an osteogenic phenotype within the lesion cells from the area were laser dissected and

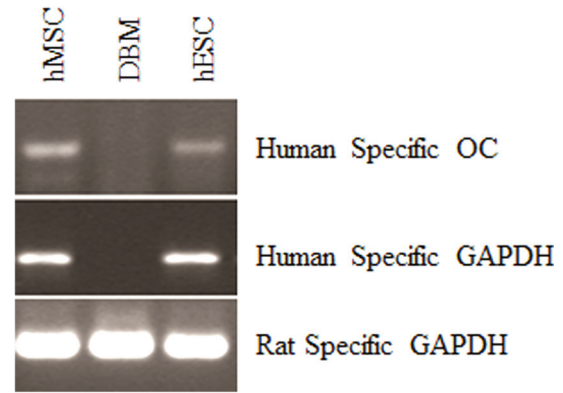


**Figure 4.** RT-PCR analysis of human osteocalcin expression in laser micro-dissected pieces collected from cryosections from the calvarial defect site (see depicted area by arrow) in immunodeficient rats after 14 days of implantation of hESC or hBMSC derived osteoprogenitor cells with or implanted with DBM alone. rGAPDH levels, human and rat specific, are shown as per control for the housekeeping gene expression.

analysed for human specific osteocalcin (osteoblast specific) mRNA's. Cryosections of the calvarial defect from the immunocompromised rats containing test cells in DBM or DBM alone for 14 days (n=3 animals per group) were prepared. A total of 25, 7  $\mu\text{m}$  cryosections were collected on RNase free PEN membrane slides (P.A.L.M. Microlaser Technologies, Germany) and fixed in 70% Ethanol prior to Eosin staining. Laser capture microdissection (LCM) was performed using PALM Robo Software (P.A.L.M. microlaser technologies) mounted on a Zeiss Axiovert 200/200 m microscope (Carl Zeiss Ltd, UK). LCM was used to specifically collect cells from within the defect site (Figure 4). Total RNA was extracted from the LCM material using RNeasy Micro Kit (Qiagen Ltd, UK) with an on column DNase treatment according to the manufacturer's instructions. RNA was accurately quantified using Nanodrop® ND-1000 spectrophotometer (Nanodrop Technologies, Inc., USA) and quality assessed using Agilent Bioanalyser. 10 ng total RNA was amplified and reverse transcribed using the WT-Ovation Kit (NuGen Technologies, Inc., USA) according to manufacturer's instructions.

The primers used in the PCR reaction were designed to be specific for Human GAPDH.

Sense 5'-ATGGATTTGGTTGTATTGGGC-3', Antisense 5'-CTAGGCAGTTGGTGGTTCAGG-3' (accession number XR\_018455) and Rat GAPDH Sense 5'-CAGTGCCAGCCTCGTCTCATA-3', Antisense 5'-GACTGTGCGTTGAACCTGCC-3' (accession number NM\_017008) and Human Osteocalcin Sense 5'-AGCCCTCACACTCCTCGC-CCC-3', Antisense 5'-GCTCACACACCTCCCTCCTGG-3' (accession number NM\_199173.2). PCR reactions were set up using Platinum Taq DNA Polymerase (Invitrogen) following manufacturers instructions. Standard PCR conditions were as follows: 2 min at 94°C; followed by 35 cycles of 50 sec denaturation at 94°C, 1 min annealing at either 65°C (Rat GAPDH, Human Osteocalcin) or 60°C (Human GAPDH).

### *Immunohistochemistry for Blood Vessel Density Count*

Rapid vascularisation of a repairing lesion will be important in order to support implanted cells. The distribution of neovascularisation will be relevant to the distribution and engraftment of implanted cells. Vessels were identified using the factor VIII-related antigen/von Willebrand's factor (vWF), a commonly used marker for vascular endothelial cells<sup>27</sup>. A subset of fixed cryosections was PBS washed and incubated with proteinase K (DakoCytomation Ltd). Endogenous peroxidase activity was quenched with 3% H<sub>2</sub>O<sub>2</sub> and endogenous biotin and biotin-related substances were blocked using the Vectastain Avidin/Biotin Blocking Kit (Vector Laboratories Ltd., Peterborough, UK) followed by a protein block (DakoCytomation Ltd). Sections were incubated with a rabbit anti-human von Willebrand (vWF) antibody (1:300; Dakocytomation Ltd), rinsed in PBS and incubated with goat anti-rabbit biotinylated IgG (1:300; Dakocytomation). Immunoreactivity was detected using avidin-biotin/peroxidase reaction (ABC Vectorstain<sup>®</sup> kit, Vector Laboratories) and visualised by diaminobenzidine tetrahydrochloride (DAB) substrate (Dakocytomation). Sections were counterstained with 0.5% (w/v) methyl green solution (Sigma-Aldrich) nuclear stain. To assess microvessel density, 6 standard fields of view (0.88 mm<sup>2</sup>) were analysed from two representative cryosections/animal using the x200 magnification in a Nikon Eclipse E800 microscope. The vWF-positive vessels were counted and the microvessel density (MVD) was calculated as the mean of these counts per mm<sup>2</sup> for each experimental group.

### *Nick-Translation assay for in situ analysis of cell apoptosis*

Active death of implanted cells in the lesion site represents one of the indicators of cell deletion. We have identified apoptotic cells within the lesion in both immunocompromised and immunocompetent animals. The percentage of cells within the defect area demonstrating significant levels of DNA fragmentation, a characteristic of apoptosis, was determined using the previously described DNA nick-translation technique<sup>28</sup>. Briefly, a subset of cryosections collected at 14 days after implantation were fixed in 4% paraformaldehyde, demineralised in 0.25 mol/L ethylenediaminetetraacetic acid (EDTA; pH 7.4) and washed 3x in PBS, and subsequently incubated in the nick-translation mix (3 mmol/L digoxigenin [DIG]-11-dUTP; 3 mmol/L each of dGTP, dATP, and dCTP, 50 mmol/L Tris HCl, pH 7.5; 5 mmol MgCl<sub>2</sub>; and 0.1 mmol/L dithiothreitol and 0.5mL/100mL DNA polymerase I) for 45 min at 37°C. Sections were incubated with fluorescein isothiocyanate (FITC)-labeled anti-DIG antibody (all from Roche Diagnostics Ltd.) and 5% normal sheep serum in PBS for 1 h at RT. Sections were counterstained with DAPI and mounted in Dako Fluorescent Mounting Medium (Dakocytomation Ltd) and visualised as described above. Positive controls were treated with DNase (0.2 mg/L in PBS; Sigma). Negative control sections were treated with the nick-translation mix in the absence of DNA polymerase I. Quantitative determinations of the apoptosis were made by counting the number of positive cells from 8 regions of each cryosections (2 cryosections/animal) under x200 magnification in a Nikon Eclipse E800 microscope. The

apoptosis index was expressed by the percentage of NT-positive cells per total number of DAPI labelled cells, which was calculated by using the ImageJ processing software (NIH, US). The overall mean values of % apoptosis were obtained per each experimental group after 14 days of implantation and data were expressed as mean±SE.

### *Quantification of mineralisation*

De novo tissue generation in the early days of a repair are important to the final outcome. Despite using a short time period in this study we have measured new bone formation over the 14 days experimental period as an indicator of lesion health. Mineralised tissue was identified using Von Kossa staining<sup>29</sup>. Fixed cryosections were incubated with 0.5% (w/v) silver nitrate under strong light for 1 hour at room temperature. Following a wash with distilled water, the sections were incubated in 5% (w/v) sodium thiosulphate. In order to visualise nuclear DNA, and establish cell presence within the defect, the sections were incubated with 4,6-diamino-2-phenylindole (DAPI) (0.1 µg/ml), washed and mounted in DakoCytomation Fluorescent Mounting Medium (DakoCytomation Denmark A/S, Denmark). Mineralised tissue was visualised as a brown/black staining and areas of newly formed woven bone could be identified<sup>30</sup>. Histomorphometric analysis was carried out on 10 representative cryosections which were randomly selected through the defect in each experimental animal, stained with Von Kossa and DAPI and examined at x200 magnification with a Nikon Eclipse E800 epifluorescent microscope (Nikon UK Ltd, Kingston upon Thames, UK). Photomicrographs were used to measure the total new bone formed at the margins and within the defect. A circular graticule was superimposed with its center positioned in the midpoint along the defect edge (Figure 2A) and the total new mineralised tissue formed within those areas and in the center of the defect was calculated using Bioquant Osteo I digital imaging analysis program (Bioquant Image Analysis Corporation, US).

### *Statistical analysis*

Statistical analysis was performed using a statistical package (SPSS 14.0<sup>®</sup> Windows; SPSS Inc, USA). Comparison of mean values and variance of the histomorphometry data for bone formation, microvessel density data and the apoptotic index between experimental groups (DBM alone, hESCs+DBM and hMSCs+DBM) for each implantation time and animal strain were analysed by one-way analysis of variance (ANOVA) with Bonferroni corrections. The different treatments between the animal strains (two group datasets) were compared with the use of unpaired Student's *t* tests. The critical level of statistical significance chosen was *P*<0.05.

## **Results**

### *Gross analysis of the calvarial defects*

No adverse clinical signs were detected following implantation of the human cells and/or DBM during the two week experimental period. At necropsy days 7 and 14 post-surgery

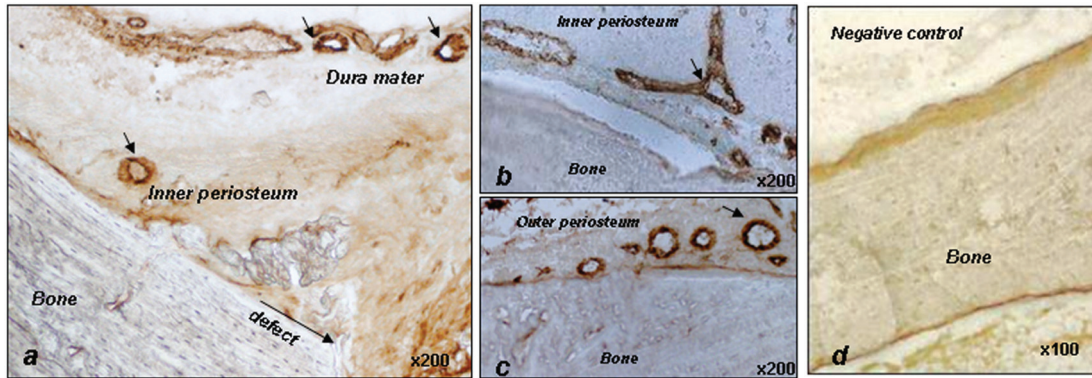


**Figure 5.** Detection of microvessels by using the VIII-related antigen/von Willebrand's factor (vWF) for vascular endothelial cells. **A)** Day 14 implanted hESC OS-derived cells in a WT rat, positive vWF stained microvessels displayed in the inner periosteum and in the dura mater (see arrows) ( $\times 200$ ). **B, C)** vWF labelled microvessels identified in the inner and outer periosteum in a day 14 OS-derived hESC implanted nude rat ( $\times 200$ ). **D)** No specific vWF staining was seen in negative controls. ( $\times 100$ ).

the gross morphological analysis of the skull showed filling of the calvarial defect for all of the implants analysed.

#### *Histological analysis of transplanted calvarial lesions*

Cryostat sections were examined for general morphology (using H&E), cellularity (DAPI) and mineralised tissue (Von Kossa).

Animals in all the treatment groups showed areas of new mineralised woven bone tissue within the lesion. No complete filling of the defect was observed after 14 days implantation of either DBM or hES or hBMS osteoprogenitor derived cells with DBM (Figures 1A, B, C), as expected in such an early post-implantation time.

By day 7 post-implantation, osteogenic activity was identified in all the groups in the form of woven bone detected commonly at the margins of the defect and migrating inwards from the endocranial margins of the defect edge (Figure 1D). The defect was filled with connective tissue, incorporating large numbers of mononuclear cells associated with the DBM particles and the bony edges. In both nude and WT animals (Figures 1A and 1B, respectively), cells were distributed throughout the whole defect area associated with loosely organised connective tissue.

By day 14, the defect area in both nude and WT animals was extensively filled with cells, with only small remnants of fibrin glue deposit. A large number of cells were concentrated on the bone margins and in the remnants of haversian canals within the DBM particles (Figure 1F). At this stage (14 days), the appearance of new mineralised areas of woven bone were observed not only on the margins but also extending towards the center of the defect, to a greater extent than at the earlier time point (Figure 1C). Some small islands of osteoid and related woven bone were also detected in the center of the defect (Figures 1E, G). Integration of the implant was evidenced by the formation of osteoid bridging between DBM particles and bony regenerate at the margins of the calvarial bone (Figure 1H).

#### *Histomorphometric examination for bone formation*

Bone formation at these early stages was measured as an indication of lesion health. Ten representative cryosections per animal from each of the total of 36 rats used (18 nude and 18 wild types) were used for histomorphometric analysis. The area of newly formed mineralized bone generated ( $\mu\text{m}^2$ ) after the implantation of DBM with or without hESC or hMSC osteoprogenitor derived cells is shown in Figure 2. 7 days after implantation of hMSC or hESC derived osteoprogenitor cells into WT rats new bone formation was not statistically different from control (DBM) groups ( $P=0.144$ ; Figure 2B). In contrast, in nude rats implantation of hESC derived cells increased significantly the amount of bone formed in the lesions relative to that in the hMSC or controls (DBM) groups ( $P<0.003$ ; Figure 2B).

In nude rats, at day 14, a significant increase in the presence of new bony regenerate was associated with implantation of both hESC and hMSC derived cells, as compared to that observed with DBM alone ( $P<0.02$ ). At this time point there was no significant difference between the hESC and hMSC treatments.

No differences were detected in bone formation in any treatment groups in WT rats.

#### *Detection of transplanted human osteoprogenitor derived cells*

To determine the survival of the implanted human cells, tissue cryosections were collected at days 7 and 14-post implantation and FISH using whole human genome probes was used to identify the human cells in the host lesion. Human ESC and MSC derived cells were detected within the defect area in both WT and nude rats following 7 days implantation. Human cells were seen sparsely scattered throughout the defect lesion in close proximity to host cells (Figure 3A, B) and appeared to be in intimate contact with the DBM particles (Figure 3D). At day 14, both hESC and hMSC derived cells were detected within the defect area in immune compromised animals (Figure 3E) while, in contrast, they were not detected in immuno-

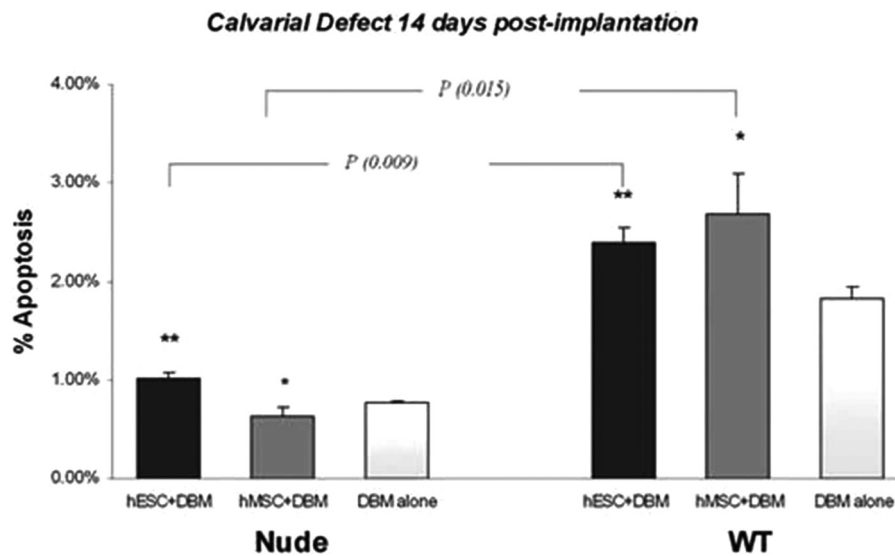


**Figure 6.** Detection of apoptotic cells using the nick-translation method for fragmented DNA. Graph bars showing the percentage of apoptotic cells detected per experimental group implanted with hBMSC or hESC OS-derived cells with DBM or DBM alone, from both strains after 14 days of surgery ( mean percentage of total cells displaying positive staining for fragmented DNA±SEM). Implantation of hESC or hBMSC OS-derived with DBM led to a 2.5 fold increase in the percentage of apoptotic cells in WT rats compared to that for nude rats (hES+DBM, P=0.009; hBMSC+DBM, P=0.015). This response was not observed when DBM alone was implanted in both nude or WT rats (P=0.1) (*t* tests  $P < 0.05$  significant differences between WT and nude rats per experimental group); No significant differences were detected between treatments within WT or nude rats. (ANOVA with Bonferroni post-hoc test;  $P < 0.05$ ).

competent animals. In immune compromised animals human cells were also detected embedded within the boney regenerate forming in the edges of the defect (Figure 3C).

#### *Transplanted human cells express osteogenic marker after 14 days transplantation*

RT-PCR analysis for human specific osteocalcin was used to determine whether an osteoblastic phenotype had been maintained in the surviving human derived cells. Expression of the human form of the osteoblast specific marker osteocalcin was detected in cells following LCM within the calvarial defect transplanted with either hESC or hMSC-derived osteoprogenitors in immunodeficient nude rats at day 14 (Figure 4).

In contrast, human specific osteocalcin mRNA expression was not detected within the calvarial defect implanted with DBM alone (Figure 4).

#### *Assessment of angiogenesis*

All samples analysed contained blood vessels that could be detected by the endothelial marker vWF at day 7 and day 14 post-implantation, displaying similar patterns of vascularity, with high density of microvessels in the calvarial inner periosteum area adjacent to the dura mater and within the other meningeal layers (Figures 5A, B), and in the outer periosteum (Figure 5C). Vessel density was lower in the central areas within the defect. No significant differences were found in the vessel density between the experimental groups at either implantation time [Day 7 (n=3, P=0.403 for WT; n=3, P=0.836

for Nude)] [Day 14 (n=3, P=0.485 for WT; n=3, P=0.597 for Nude)].

#### *Cell implantation in immune competent rats is associated with apoptosis*

In order to assess general loss of cells in the lesion site of both WT and nude animals, cellular apoptosis was studied. Cell apoptosis was demonstrated *in situ* using a Nick-Translation technique (Figure 6). Negative controls showed no DIG labelling while extensive numbers of positive DIG labelled cells (green blended with blue/Dapi staining) were seen in the positive controls. Apoptotic cells were detected in all the experimental groups from both strains after 14 days of surgery. The percentage of apoptotic cells in the lesion at 14 days was found to be 2.5 times higher in the WT than in the immune-deficient animals when cells were implanted with DBM. This difference was not observed when DBM alone was implanted in either nude or WT rats (P=0.1) (Figure 6). Within the same animal strain, the percentages of apoptosis did not differ between the animals implanted with cells derived from hES or hMSC together with DBM, or implantation of DBM alone. (P=0.453 for WT; P=0.374 for Nude) (Figure 6). Apoptotic cells were distributed throughout the implanted/healing area.

## **Discussion**

Here we provide evidence that osteoprogenitor cells derived through directed differentiation from hESCs can survive, main-

tain an osteoblastic phenotype and support the initiation of bone regeneration following transplantation into a calvarial defect in an immunocompromised animal model in a similar pattern to that observed by hMSCs derived osteoprogenitor cells.

Bone marrow derived stromal cells from a variety of species (human<sup>19</sup>, rat<sup>25</sup>, rabbit<sup>31</sup> mice<sup>32</sup>, sheep<sup>33</sup>) have been used in the regeneration of calvarial defects. However, reports on bone regeneration using hES derived osteoprogenitor cells are limited and results remain inconsistent. While most of the *in vivo* studies showed that osteoprogenitor cells derived from hESCs were able to promote the production of discrete areas of ectopic mineralised tissue after ectopic implantations<sup>13-15,17</sup>, studies following implantation in an injured orthotopic site<sup>16</sup> are scarce and they showed that transplanted cells did not regenerate enough bone to bridge the critical size bone defect. Such findings raise concerns on the survival of hESC derived cells following implantation and that their fate may be compromised by the health status of the injury site such as poor blood supply causing hypoxia and delayed angiogenesis. *In vivo* models remain a critical tool for testing the feasibility of a new therapeutic approach, and some challenges are presented relating to the transplantation of human cells into animals. Whenever possible, the intended human stem cell product should be used for efficacy and safety studies and the use of immune-compromised animals should be considered to prevent rejection of the human cellular product<sup>34</sup>. However, the immune issues related to xenotransplantation models can make extrapolation to humans difficult. Therefore it is important to critically determine the particular outcomes that are relevant to a particular animal model<sup>35</sup>. The calvarial defect model provides the appropriate anatomic location and a reproducible approximation of the real-life *in vivo* settings for assessing the short-term fate of various culture-differentiated and expanded osteoprogenitor cell populations. In particular, the present study demonstrates that hES derived osteoprogenitor cells were able to engraft and survive *in vivo* in a similar pattern as the hBMS derived osteoprogenitors during the initial two week period following implantation, maintaining their differentiation status as detected by gene expression and by supporting regeneration in an experimental bone defect in immuno-deficient animal model. Our histological data supports the formation of bone nodular patterns largely in the periphery of the calvarial defect as shown by others<sup>17</sup> but bone formation was also observed around some DBM carrier particles within the defect area. Furthermore, our histological findings showed the presence of human cells immerse within newly formed bony matrix, together with other cells from recipient origin. At this stage, it would be difficult to fully predict the long term functionality of these cells and their interaction to promote further remodelling of the woven bone towards well-structured lamellar bone. However, it is encouraging to detect human cells well integrated within the implantation site. Furthermore, the study provides experimental evidence of the efficacy of survival and engraftment of cells in an effective clinically relevant setting for assessing bone repair. This supports the rational selection and use of an appropriate animal model (e.g. orthotopic im-

plantation, immunocompromised model) as a valuable preclinical model to investigate bone regeneration and elucidate further clues on the clinical relevance for testing stem cell implantation based therapies.

In the current studies hESC and hMSC derived osteoprogenitor cells were implanted in combination with a demineralised bone matrix carrier. When introduced into lesions in immune compromised animals test cells of both adult and embryonic derivation were capable of detectable levels of viability and functionality. Such response was not observed when implanted into WT, as expected due to the cell rejection response. Indeed, nude rats only possess a rudimentary thymic tissue, with a reduced number of T lymphocytes<sup>36</sup> which conveys a certain level of immunological tolerance to these animals. Cells have been found to undergo apoptosis when exposed to inflammatory cytokines produced by activated immune cells such as T-lymphocytes<sup>37</sup>; this immune-mediated apoptosis is likely to be reduced in the nude rats and would explain the different cell survival and function to support bone formation between nude and WT animals. In fact by day 14 it is very likely that most of the bone formed may be related to the creeping substitution response and the DBM support, with little participation of the implanted progenitor cells. On this vein, a potential use of strategies for supporting cell survival and angiogenic activity may enhance further survival of implanted cells<sup>38</sup>.

Previous studies have demonstrated that DBM is moderately osteoinductive<sup>39</sup> and it has been extensively used clinically to supplement areas of bone loss<sup>40-42</sup>. Moreover, the innate repair of calvarial defects in the presence of DBM occurs primarily by the direct induction of osteoblasts via the intramembranous ossification pathway rather than via an endochondral pathway<sup>43</sup>. In the current study, histological analysis revealed good cellular integration of the implanted DBM with or without test cells, supporting its role as a good osteoconductive carrier. Implanted human derived osteoprogenitor cells were seen to be closely interacting with the DBM particles, and bony bridging between the DBM particles and the edges of the host calvarial bone was also observed, indicating a high degree of biocompatibility with the DBM material. However, when the DBM was implanted alone, a significant amount of apoptosis was still detected in the WT animals, indicating the limited tolerance following transplantation of xenogeneic material in these animals. Such remarkable apoptotic responses were not observed in nude rats which is likely related to the differing characteristics of their immune systems, as previously discussed.

The fact that the addition of hESC in DBM to immune compromised animals supported the early (within 7 days) bone formation relative to DBM containing hMSC may point to a different behaviour in the initial response following *in vivo* implantation for the two cell sources. Interestingly, our earlier work would suggest a similar propensity for bone formation by the two cell sources, hESCs and hMSCs, *in vitro*<sup>12</sup>. On the other hand, in recent work in our laboratories, bone formation within diffusion chambers at an ectopic site did appear more

efficacious using hESC relative to hMSC<sup>14</sup>. The lack of an early response to hMSCs may be due to the higher heterogeneity of the initial unsorted marrow stromal cell cultures<sup>44</sup>.

The difference in persistence of cells of both derivations when implanted in immune competent animals relative to those in immune compromised animals points to the ability of both to illicit an immune response resulting in immune rejection. Xenoreactivity and its influence on engraftment of the implanted human cells into the animal lesion are important considerations in the use of animal models in the development of a cell based therapy<sup>45</sup>. Despite some reports pointing to a reduced immunogenicity of hMSC and hESC and an immune suppressive activity of hMSC<sup>46</sup>, it is important to recognise that future therapies will more commonly comprise differentiated cells derived from stem cell populations and hence any potential acquisition of immunogenicity with differentiation is relevant<sup>47</sup>. hMSCs can be recognized by alloreactive T cells since they express intermediate levels of human leukocyte antigen (HLA) major histocompatibility complex (MHC) class I molecules and can be induced by interferons (IFNs) to express HLA class II<sup>48</sup>. Following osteogenic differentiation these hMSCs express MHC class I but no longer class II<sup>46</sup>, maintaining their xenoreactivity<sup>49</sup>. Undifferentiated hESCs only express low levels of MHC-I molecules<sup>50,51</sup>, while differentiation *in vitro* upregulates MHC-I expression. MHC-II is not expressed under these conditions<sup>51</sup>. Despite these low levels of MHC-I, hESCs and their differentiated derivatives remain susceptible to T cell recognition after transplantation. It is quite likely that the immunogenicity of the hESC differentiated derivatives increases after transplantation as cells mature further, as demonstrated by Swijnenburg et al.<sup>52</sup>. From our study, and in accordance with these findings, while it was clear that human cells persisted in WT for 7 days; longer term survival is unlikely to occur after xenotransplantation.

Consistent with a stable directed differentiation, no side effects or initiation of tumour formation were detected after the short-term transplantation of differentiated cell derivatives from either hESCs or hMSCs. However, longer time points of implantation would be needed to determine the formation of teratoma. Anatomically the bulk of the regeneration occurred from the edges of the defect. Interestingly, at early time points, bone formation was most evident in the internal site of the calvarial edge area close to the dura matter. Studies in calvarial morphogenesis have reported an interaction between the juvenile dura matter and the cranial osteoblast during bone induction and calvarial reossification<sup>53</sup>, and similar bone regeneration patterns were reported by Cowan et al.<sup>54</sup> in a calvarial defect following implantation of mouse adipose-derived stromal cells. In the current study, within the two week period, the bone formation progressed further towards the centre of the defect mostly from the inner pericranial edges of the bone in all the groups. Limited bone formation was detected on the ectocranial side of the defect which may be associated with the fact that the periosteum was peeled away from the lesion. Periosteum provides both blood supply to cortical bone and osteoprogenitor cells for bone regeneration<sup>55</sup>; thus, timely

blood vessel in-growth must be initiated to promote healing and ossification<sup>56</sup>. The vascular patterns, observed in our study, although no differences were detected between groups, correlate with the bone regeneration patterns described on calvarial reossification, with a remarkable vascular density in the inner periosteum area adjacent to the dura mater and within the other meningeal layers. This delay for bone formation to occur in the centre of the defect might be related to the longer time required for vascular invasion to reach the more central sites and also to the rapid in-growth of the pericranial fibrous tissue which may restrict the osteogenic properties of the adjacent dura and pericranium<sup>57,58</sup>.

Human osteocalcin was used to demonstrate the presence of human osteoblasts in the defect. Osteocalcin remains the selected marker to identify mature osteoblasts with bone forming capacity and not early osteogenic progenitor cells. Hence we will not have detected all of the early osteogenic precursor cells but rather the more mature cells. Osteocalcin expression in the engrafted hESC and the deposition of mineralized nodules in the defect represent the two main specific features of bone differentiation supporting the functional role of the implanted human derived cells *in vivo* within a bone defect area. This approach was taken to gather further information of the characterisation of the implanted human cells that remain viable and engrafted in the defect by day 14 post-implantation. Despite the detection of human cells embedded within the woven bone, the discrimination of bone material directly produced by the human cells was technically challenging due to the limited specificity of human markers such as collagen type I, being picked up by all the host bone.

This study confirms previous work regarding the osteogenic capacity of hMSC and hESCs but more importantly demonstrates that osteoprogenitor cells derived from hESCs can successfully survive and engraft following xenotransplantation in an orthotopic site and thus successfully support the initial the repair of bone *in vivo*. Our histomorphometric data relating to the identification of implanted human cells and gene expression support the survival and the functional role of these hESC cells in a similar manner as the hMSCs. Our findings also highlight the importance of undertaking such *in vivo* implantation studies in appropriate injury site and using the immuno-compromised animals. The fact that no remarkable differences on survival and engraftment were observed between the hESCs and the hMSCs progeny at this early stage of implantation, may elucidate further directions towards supporting the osteogenic potential of the hESC derived cells, possibly through the development of bioactive scaffolds that may help to support their osteogenic function in a longer term. At this stage, it is also difficult to specifically discriminate between a direct or indirect positive effect of the implanted osteoprogenitor cells on the host cells. Nevertheless, the engraftment of the human cells and their support of bone formation demonstrated in this study emphasize the need to continue these preclinical studies to develop a robust methodology for bringing these stem-cell based therapies into skeletal regenerative medicine.

### Acknowledgements

Dr C. Huber is gratefully acknowledged for her assistance with the Nick-Translation assays and Miss A. Voultsiadou for her advice with the laser capture microdissection. Funding is gratefully acknowledged from Geron Corporation and from the UK Medical Research Council (MRC-Grant No GO300287).

### References

- Bolland BJ, Tilly S, New AM, Dunlop DG, Oreffo RO. Adult Mesenchymal stem cells and impacting grafting a new clinical paradigm shift. *Expert Dev Med Devices* 2007;4:393-404.
- Cancedda R, Dozin B, Giannoni P, Quarto R. Tissue engineering and cell therapy of cartilage and bone. *Matrix Biol* 2003;22:81-91.
- Dimitriou R, Jones E, McGonagle D, Giannoudis PV. Bone regeneration: current concepts and future directions. *BMC Med* 2011;31:9:66.
- Bianco P, Robey PG. Stem cells in tissue engineering. *Nature* 2001;414:118-21.
- Mendes SC, Tibbe JM, Veenhof M, Bakker K, Both S, Platenburg PP, Oner FC, de Bruijn JD, van Blitterswijk CA. Bone tissue-engineered implants using human bone marrow stromal cells: effect of culture conditions and donor age. *Tissue Eng* 2002;8:911-20.
- Horwitz EM, Gordon PL, Koo WW, Marx JC, Neel M, McNall RY, Muul L, Hofmann T. Isolated allogeneic bone marrow-derived mesenchymal cells engraft and stimulate growth in children with osteogenesis imperfecta: Implications for cell therapy of bone. *Proc Natl Acad Sci USA* 2002;99:8932-7.
- Meijer GJ, de Bruijn JD, Koole R, van Blitterswijk CA. Cell based bone tissue engineering in jaw defects. *Biomaterials* 2008;29:3053-61.
- Friedenstein AJ, Piatetzky-Shapiro II, Petrakova KV. Osteogenesis in transplants of bone marrow cells. *J Embryol Exp Morphol* 1966;16:381-90.
- Quarto R, Mastrogiacomo M, Cancedda R, Kutepov SM, Mukhacher V, Lavroukov A, Kon E, Marcacci M. Repair of large bone defects with the use of autologous bone marrow stromal cells. *N Engl J Med* 2001;344:385-6.
- Muschler GF, Nitto H, Matsukura Y, Boehm C, Valdevit A, Kambic H, Davros W, Powell K, Easley K. Spine fusion using cell matrix composites enriched in bone marrow-derived cells. *Clin Orthop Relat Res* 2003;407:102-18.
- Bonab MM, Alimoghaddam K, Talebian F, Ghaffari SH, Ghavamzadeh A, Nikbin B. Aging of mesenchymal stem cells *in vitro*. *BMC Cell Biol* 2006;7:14.
- Sottile V, Thomson A, McWhir J. *In vitro* osteogenic differentiation of human ES cells. *Cloning Stem Cells* 2003; 5:149-55.
- Bielby RC, Boccaccini AR, Polak JM, Buttery LD. *In vitro* differentiation and *in vivo* mineralization of osteogenic cells derived from human embryonic stem cells. *Tissue Eng* 2004;10:1518-25.
- Tremoleda JL, NR Forsyth, Khan N, Wojtacha D, Christodoulou I, Tye BJ, Racey SN, Collishaw S, Sottile V, Thompson AJ, Simpson AH, Noble BS, McWhir J. Bone tissue formation from human embryonic stem cells *in vivo*. *Cloning Stem Cells* 2008;10:119-32.
- Kim S, Kim SS, Lee SH, Ahn SE, Gwak SJ, Song JH, Kim BS, Chung HM. *In vivo* bone formation from human embryonic stem cell-derived osteogenic cells in poly (d,L-lactic-co-glycolic acid)/hydroxyapatite composite scaffolds. *Biomaterials* 2008;29:1043-53.
- Arpornmaeklong P, Brown SE, Wang Z, Krebsbach PH. Phenotypic characterization, osteoblastic differentiation, and bone regeneration capacity of human embryonic stem cell-derived mesenchymal stem cells. *Stem Cells Dev* 2009;18:955-68.
- Kuznetov SA, Cherman N, Robey PG. *In vivo* bone formation by progeny of human embryonic stem cells. *Stem Cells and Development* 2011;20:269-87.
- Muschler GF, Raut VP, Patterson TE, Wenke JC, Hollinger JO. The design and use of animal models for translational research in bone tissue engineering and regenerative medicine. *Tissue Engineering part B* 2010; 16:123-45.
- Mankani MH, Kuznetsov SA, Wolfe RM, Marshall GW, Robey PG. *In vivo* bone formation by human bone marrow stromal cells: reconstruction of the mouse calvarium and mandible. *Stem Cells* 2006;24:2140-9.
- Thomson JA, Itskovitz-Eldor J, Shapiro SS, Waknitz MA, Swiergiel JJ, Marshall VS, Jones JM. Embryonic stem cell lines derived from human blastocysts. *Science* 1998; 282:1145-7.
- Löser P, Schirm J, Guhr A, Wobus AM, Kurtz A. Human Embryonic Stem Cell Lines and Their Use in International Research. *Stem Cells* 2010;28:240-6.
- Xu C, Inokuma MS, Denham J, Gods K, Kundu P, Gold JP, Carpenter MK. Feeder-free growth of undifferentiated human embryonic stem cells. *Nat Biotechnol* 2001; 19:971-4.
- McWhir J, Wojtacha D, Thomson A. Routine culture and differentiation of human embryonic stem cells. *Methods Mol Biol* 2006;331:77-90.
- Haynesworth SE, Goshima J, Goldberg VM, Caplan AI. Characterization of cells with osteogenic potential from human marrow. *Bone* 1992;13:81-8.
- Gurevith O, Kurkalli BG, Prigozhina T, Gaft A, Slavin S. Reconstruction of cartilage, bone, and hematopoietic microenvironment with demineralised bone matrix and bone marrow. *Stem Cells* 2003;21:588-97.
- Newsome PN, Johannessen I, Boyle S, Dalakas E, McAulay KA, Samuel K, Rae F, Forrester L, Turner ML, Hayes PC, Harrison DJ, Bickmore WA, Plevris JN. Human cord blood-derived cells can differentiate into hepatocytes in the mouse liver with no evidence of cellular fusion. *Gastroenterology* 2003;124:1891-900.
- Weidner N, Semple JP, Welch WR. Tumour angiogenesis

- and metastasis-correlation in invasive breast carcinoma. *N Engl J Med* 1991;324:1-8.
28. Noble BS, Stevens H, Loveridge N, Reeve J. Identification of apoptotic changes in osteocytes in normal and pathological human bone. *Bone* 1997;20:273-82.
  29. Bills CE, Eisenberg H, Pallante SL. Complexes of organic acids with calcium phosphate: the von Kossa stain as a clue to the composition of bone mineral. *Johns Hopkins Med J* 1971;128:194-207.
  30. Walsh WR, Walton M, Bruce W, Yan Y, Gillies RM, Svehla M. Cell structure and biology of bone and cartilage. In *Handbook of histology methods for bone and cartilage*. 2003, Ed An YH, Martin KL Humana press.
  31. Yew TL, Huang TF, Ma HL, Hsu YT, Tsai CC, Chiang CC, Chen WM, Hung SC. Scale-up of MSC under hypoxic conditions for allogeneic transplantation and enhancing bony regeneration in a rabbit calvarial defect model. *J Orthop Res* 2012;30:1213-2.
  32. Krebsbach PH, Mankani Mh, Satomura K, Kuznetsov SA, Robey PG. Repair of craniotomy defects using bone marrow stromal cells. *Transplantation* 1998;10:1272-8.
  33. Shang Q, Wang Z, Liu W, Shi Y, Cui L, Cao Y. Tissue-engineered bone repair of sheep cranial defects with autologous bone marrow stromal cells. *J Craniofac Surg* 2001;12(6):586-93.
  34. Frey-Vasconcells J, Whittlesey KJ, Baum E, Feigal EG. Translation of stem cell research: points to consider in designing preclinical animal studies. *Stem Cells Translational Medicine* 2012;1:1-6.
  35. Muschler GF, Raut VP, Patterson TE, Wenke JC, Hollinger JO. The design and use of animal models for translational research in bone tissue engineering and regenerative medicine. *Tissue Eng Part B Rev* 2010;16:123-45.
  36. Vos JG, Berkvens JM, Kruijt BC. The athymic nude rat. I. Morphology of lymphoid and endocrine organs. *Clin Immunol Immunopathol* 1980;15:213-28.
  37. Geng YJ, Wu Q, Muszynsky M, Hansson GK, Libby P. Apoptosis of vascular smooth muscle cells induced by *in vitro* stimulation with interferon-gamma, tumor necrosis factor-alpha, and interleukin-1 beta. *Arterioscler Thromb Vasc Biol* 1996;16:19-27.
  38. Zou D, Zhang Z, Ye D, Tang A, Deng L, Han W, Zhao J, Wang S, Zhang W, Zhu C, Zhou J, He J, Wang Y, Xu F, Huang Y, Jiang X. Repair of critical-sized rat calvarial defects using genetically engineered bone marrow-derived mesenchymal stem cells overexpressing hypoxia-inducible factor-1 $\alpha$ . *Stem Cells* 2011;29:1380-90.
  39. Hanamura H, Higuchi Y, Nakagawa M, Iwata H, Nagami H, Urist MR. Solubilized bone morphogenetic protein (BMP) from Mouse osteosarcoma and rat demineralised bone matrix. *Clin Orthop Relat Res* 1980;148:281-90.
  40. Damien CJ, Parsons JR, Prewett AB, Rietveld DC, Zimmerman MC. Investigation of an organic delivery system for demineralized bone matrix in a delayed-healing cranial defect model. *J Biomed Mater Res* 1994;28:553-61.
  41. Tiedeman JJ, Garvin KL, Kile TA, Connolly JF. The role of a composite, demineralized bone matrix and bone marrow in the treatment of osseous defects. *Orthopedics* 1995;18:1153-8.
  42. Acarturk TO and Hollinger J. Commercially available demineralised bone matrix compositions to regenerate calvarial critical-sized bone defects. *Plast Reconstr Surg* 2006;118:862-73.
  43. Wang J and Glimcher MJ. Characterization of matrix-induced osteogenesis in rat calvarial bone defects: I. Differences in the cellular response to demineralised bone matrix implanted in calvarial defects and in subcutaneous sites. *Calcif Tissue Int* 1999;65:156-65.
  44. Friedenstein AJ, Chailakhyan RK, Gerasimov UV. Bone marrow osteogenic stem cells: *in vitro* cultivation and transplantation in diffusion chambers. *Cell Tissue Kinet* 1987;20:263-72.
  45. Fairchild PJ, Cartland S, Nolan KF, Waldmann H. Embryonic stem cells and the challenge of transplantation tolerance. *Trends Immunol* 2004;25:465-70.
  46. LeBlanc K, Tammik C, Rosendahl K, Zetterberg E, Ringdén O. HLA Expression and immunologic properties of differentiated and undifferentiated mesenchymal stem cells. *Exp Hematology* 2003;890-96.
  47. Bradley JA, Bolton EM, Pedersen RA. Stem Cell medicine encounters the immune system. *Nat Rev Immunol* 2002;2:859-71.
  48. Tse WT, Pendleton JD, Beyer E, Egalka MC, Guinan EC. Suppression of allogeneic T-cell proliferation by human marrow stromal cells: implications in transplantation. *Transplantation* 2003;75:389-97.
  49. Grinnemo KH, Månsoon A, Dellgren G, Klingberg D, Wardell E, Drvota V, Tammik C, Holgersson J, Ringdén O, Sylvén C, Le Blanc K. Xenoreactivity and engraftment of human mesenchymal stem cells transplanted into infarcted rat myocardium. *J Thorac Cardiovasc Surg* 2004;127:1293-300.
  50. Drukker M, Katz G, Urbach A, et al. Characterization of the expression of MHC proteins in human embryonic stem cells. *Proc Natl Acad Sci USA* 2002;99:9864-9.
  51. Drukker M, Katchman H, Katz G, Friedman Even-Tov S, Shezen E, Hornstein E, Mandelboim O, Reisner Y, Benvenisty N. Human embryonic stem cells and their differentiated derivatives are less susceptible to immune rejection than adult cells. *Stem Cells* 2006;24:221-9.
  52. Swijnenburg RJ, Tanaka M, Vogel H, Baker J, Kofidis T, Gunawan F, Lebl DR, Caffarelli AD, de Bruin JL, Fedoseyeva EV, Robbins RC. Embryonic stem cell immunogenicity increases upon differentiation after transplantation into ischemic myocardium. *Circulation* 2005;112:1166-72.
  53. Greenwald JA, Mehrara BJ, Spector JA, Warren SM, Crisera FE, Fagenholz PJ, Bouletreau PJ, Longaker MT. Regional differentiation of cranial suture-associated dura mater *in vivo* and *in vitro*: implications for suture fusion and patency. *J Bone Miner Res* 2000;15:2413-30.
  54. Cowan CM, Shi Y-Y, Salami OO, Chou YF, Mari C,

- Thomas R, Quarto N, Contag CH, Wu B, Longaker MT. Adipose-derived adult stromal cells heal critical-size mouse calvarial defects. *Nature Biotech* 2004;22:560-7.
55. Eyre-Brook AL. The periosteum: its function reassessed. *Clin Orthop Relat Res*;189:300-7.
56. Einhorn TA. The cell and molecular biology of fracture healing. *Clin Orthop* 1998;355:S7-S21.
57. Hopper RA, Zhang JR, Fournasier VL, Morova-Protzner I, Protzner KF, Pang CY, Forrest CR. Effect of isolation of periosteum and dura on the healing of rabbit calvarial inlay bone grafts. *Plast Reconstr Surg* 2001;107:454-62.
58. Gossain AK, Santoro TD, Song LS, Capel CC, Sudhakar PV, Matloub HS. Osteogenesis in calvarial defects: contribution of the dura, the pericranium, and the surrounding bone in adult versus infant animals. *Plast Reconstr Surg* 2003;112:515-27.